Soils and Foundations 2015;55(2):227–241

HOSTED BY

ELSEVIER

CrossMark

The Japanese Geotechnical Society

Soils and Foundations

www.sciencedirect.com

journal homepage: www.elsevier.com/locate/sandf

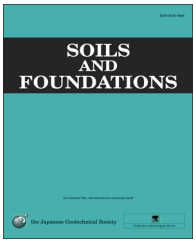


# Seismic stability and displacement analyses of earth slopes using non-circular slip surface

Masahiro Shinoda*

*Railway Technical Research Institute, 2-8-38, Hikari-cho, Kokubunji-shi, Tokyo 185-8540, Japan*

Received 28 February 2014; received in revised form 30 October 2014; accepted 18 November 2014
Available online 26 March 2015

**Abstract**

The seismic stability and deformability of earth slopes are conventionally evaluated by simple, practical methods. Because a multimodal function optimization problem makes it mathematically difficult to search large critical slip surface of earth slopes with complex strata, stability analysis is one of the classical problems of geotechnical engineering. One option is to evaluate the seismic deformability of earth slopes using permanent seismic displacements via Newmark's sliding block analysis in the current seismic design. The advantage of this method is that it is useful in practice and is less time consuming in terms of calculations. However, the calculations require that the critical slip is assumed either linear or circular. This paper proposes two methods for computing safety factors and permanent seismic displacements of earth slopes using an efficient non-circular slip surface search algorithm based on the force equilibrium given by the Spencer method. The validity of these proposed methods is verified by applying them to models with a known safety factor or theoretically calculated permanent seismic displacement and the results obtained compared. Comparative analyses are also conducted in order to demonstrate their efficacy in terms of computation precision and convergence performance. Further, they are utilized to calculate the permanent seismic displacement of a practical earth slope model subjected to seismic motions in both the horizontal and vertical directions. The results obtained indicate that they can calculate the safety factor of earth slopes using a smaller number of simulations than conventional methods and that they can also be applied to calculate the permanent seismic displacement of earth slopes. The results also indicate that the permanent seismic displacement calculated is an important index that can be used to quantitatively evaluate the seismic performance of earth slopes.


*IGS:* E- 6; E- 8; G- 6; G- 8

*Keywords:* Slope; Stability analysis; Displacement analysis; Permanent seismic displacement

## 1. Introduction

In recent years, a number of powerful earthquakes have occurred in various regions in Japan, resulting in severe damage to many embankments and earth slopes. This damage typically involves the burying of private houses and the closure of roads and railways. For example, Koseki et al. (2012) reported several case histories including the collapse of a high cut slope due to the 2011 off the Pacific Coast of Tohoku Earthquake in Japan. Hyodo et al. (2012) reported five slope failures which occurred in a residential area on artificial valley fills due to the same earthquake. Embankments and earth slopes with low seismic stability need be evaluated appropriately, either by field investigation or numerical analysis, to

*Tel.: +81 42 573 7261.
*E-mail address:* shinoda.masahiro.97@rtri.or.jp
Peer review under responsibility of The Japanese Geotechnical Society.

http://dx.doi.org/10.1016/j.sandf.2015.02.001

reduce such damage to embankments and earth slopes. To comprehensively evaluate the seismic stability of embankments, it is important to consider the construction records and factors such as ground and environmental conditions, in addition to simple field investigations, including cone penetration tests, a practical stability analysis and displacement analysis. Since no simple field investigation method has yet to be established for the seismic stability evaluation of earth slopes, practical stability and displacement analyses are essential.

Methods for evaluating the seismic stability of an earth slope using a safety factor calculated from the ratio of the sliding force and the resistive force of soil mass that follow along the slip surface in a limit equilibrium state are generally known as stability analysis methods. Stability analysis methods can be classified according to the approach they use to search the slip surface and calculate the safety factor. Methods that assume the slip surfaces are circular include the Fellenius and Bishop methods (Fellenius, 1936; Bishop, 1954). These classical methods calculate a safety factor that satisfies the force equilibrium equation under simple assumptions. They are widely used in actual practice because they are considered to generate no major errors in comparison to the exact solutions, and the safety factors that they provide are usually almost the same or slightly smaller.

There are also methods that assume that the slip surfaces are non-circular, such as the Janbu method (Janbu, 1955), the Morgenstern–Price method (Morgenstern and Price, 1965), and the Spencer method (Spencer, 1967, 1973). The Janbu method is mechanically hyperstatic (Sarma and Bhave, 1979). The Morgenstern–Price method and the Spencer method determine the safety factor by satisfying both the force and the moment equilibrium equations by considering the forces in between slices and hence, can be considered exact methods. The similarities of the Morgenstern–Price method and the Spencer method are discussed in detail by Kondo and Hayashi (1997). Although the Morgenstern–Price method is considered to be more general than the Spencer method, the computation processes of both these methods use the same equilibrium condition equations; therefore, the simpler Spencer method is more appropriate for practical applications.

Methods that calculate the permanent seismic displacement of slopes subjected to a strong ground motion using a displacement that integrates the equation of rotational motion of a soil mass contained within the critical circular slip surface are generally known as Newmark's sliding block analysis methods (Newmark, 1965). Newmark's sliding block analysis is a simplified procedure, employed in the design code of railway, road, and dam structures in Japan (RTRI, 2000; JRA, 2010; MLIT, 2005), in which the critical circular slip surface is determined using a conventional stability analysis. Newmark's sliding block analysis requires unit weight, friction angle, and soil cohesion values. The method is useful practically and less time consuming, in terms of calculations, than other methods. Newmark's sliding block analysis will be hereafter referred to as Newmark analysis.

When conducting the seismic stability analysis or Newmark analysis, as mentioned above, the slip surface must be determined. In searching for a conventional circular slip surface, the only parameters required are the arc center and the radius, which enables the easy determination of the slip surfaces. To evaluate the stability or deformability of earth slopes composed of homogenous foundation material, a seismic stability analysis or Newmark analysis using the circular slip surface is highly practical, but in evaluating the seismic stability or deformability of natural slopes that have complex strata with weak layers, the safety factors or permanent seismic displacement obtained by these methods are not always the smallest safety factors or the largest permanent seismic displacements.

On the other hand, for non-circular slip surfaces, the seismic stability or Newmark analysis methods require the setting of constraint conditions and a search for slip surfaces with a minimum safety factor or maximum permanent seismic displacement. However, while a stability analysis or Newmark analysis with non-circular slip surface can obtain reasonable slip surfaces even for natural slopes with complex strata, there are issues in relation to the complexity of its computation algorithm and the high computation cost required to obtain appropriate solutions. These problems arise because of the need to solve a multimodal function with slip surface coordinates as variables when searching the non-circular slip surface of natural slopes, resulting in the optimization of a multimodal function that satisfies the goal of a minimum safety factor.

On the basis of the above background, various optimization methods have been proposed. Early examples include the conjugate gradient method (Yamagami and Ueta, 1988), the pattern search method (Greco, 1996), and the Monte Carlo method (Greco, 1996). These methods can easily converge on local solutions depending on the initial value settings and, in some cases, may not be able to provide an appropriate optimum solution. A genetic algorithm (GA) is a typical example of a method that includes a process for searching for the optimum solution while converging on local solutions. This method has frequently been applied (Goh, 1999). Cheng et al. (2007a) applied simulated annealing, GA, particle swarm optimization (PSO), a simple harmony search, a modified harmony search, and a Tabu search to various slope models. They found that PSO had the highest practical applicability. However, although PSO is easy to implement and robust in performance, it tends to be computationally expensive for high strata earth slopes. Consequently, Shinoda (2013a) proposed an efficient PSO-based critical slip surface search algorithm with high computational precision and convergence performance.

Considering stability analysis in the presence of plain failure and circular failure, many studies have used Newmark analysis to estimate the earthquake-induced slope displacement. Currently, it is well known that Newmark analysis can be used to estimate practical slope displacement, as confirmed by Goodman and Seed (1966) and Wartman et al. (2003, 2005) in laboratory model tests, and Wilson and Keefer (1983) and Pradel et al. (2005) in analyses of earthquake-induced landslides in natural slopes. Yan et al. (1996) proposed a modified Newmark analysis method for a rigid block on an inclined plane, which incorporated the vertical component of the

seismic motion. Comprehensive reviews of the sliding block analysis procedures have been conducted by Kramer (1996), Wasowsli et al., 2011, and Jibson (2011).

Jibson (2011) classified analytical procedures used to estimate earthquake-induced slope displacements into three types: rigid-block, decoupled, and coupled. In a rigid-block analysis, a sliding block is modeled as a rigid mass that slides on an inclined plane. This analysis method assumes that there is little or no deformation of the soil mass. A decoupled analysis is more sophisticated in its approach to the deformation of the soil mass. The most commonly used decoupled analysis method was developed by Makdisi and Seed (1978). In this method, the computation of the dynamic analysis response and the plastic displacement are performed independently. In a coupled analysis, the dynamic response of the soil mass and the permanent displacement are modeled together to take the effect of plastic sliding displacement on the ground motions into account. Bray and Travasarou (2007) developed a simplified approach that uses a nonlinear, fully coupled sliding-block model to produce a semi-empirical relationship to estimate seismic displacement. Shinoda (2013b) proposed a method to calculate the permanent seismic displacement of earth slopes with non-circular slip surfaces. However, the proposed calculation method does not include a non-circular critical slip surface search algorithm for earth slopes.

It is well-known that geomaterials have non-linear characteristics exhibiting peak and residual strengths. Koseki et al. (1998) proposed a modified and pseudo-static limit-equibilium approach to evaluate active earth pressure at high seismic load levels on retaining walls. The proposed method considered associated post-peak reduction in the shear resistance from peak to residual states. Matasovic et al. (1997) proposed a trilinear model for the degradation of yield acceleration as a function of displacement implemented in the Newmark analysis. In this model, it is assumed that yield acceleration degrades linearly with increasing displacement from the peak to residual states.

In this paper, an efficient non-circular stability analysis method with a simple critical slip surface search algorithm is proposed. The safety factor computation method given by the Spencer method sets a force equilibrium equation that takes both the horizontal and vertical seismic intensity into consideration. A non-circular permanent seismic displacement analysis method based on the above critical slip surface search algorithm is also proposed. For simplicity, in this analysis, the degradation of yield acceleration is not considered. The efficacy of the proposed methods in terms of computation precision and convergence performance is verified using slope models for which the safety factors are known from past research. Finally, the paper demonstrates how the permanent seismic displacement of a realistic earth slope model subjected to horizontal and vertical seismic motions can be successfully calculated.

## 2. Objective of analysis

The principal objective of the current analysis in this paper is to propose methods for seismic performance evaluation of earth slopes. Two calculation methods are proposed: One method calculates the safety factor of the earth slopes; the other calculates the permanent seismic displacement of earth slopes subjected to ground motion in both the horizontal and vertical directions. Further, a PSO-based critical slip surface search method is proposed that allows for the critical slip surfaces of the earth slopes to be searched. The proposed methods provide precise seismic stability and displacement analysis techniques to compute a wide geometrical range of earth slopes using the non-circular critical slip surface method.

## 3. PSO-based critical slip surface search method

The PSO method is a type of probabilistic multipoint search-driven optimization method based on the herd intelligence seen in shoals of fish and flocks of birds (Kennedy and Eberhart, 1995). This method effectively solves complex non-differentiable problems, and its ease of mounting has facilitated its application to multimodal function optimization problems in a variety of fields in recent years. Researchers who previously applied PSO to slope stability analysis set its parameters uniformly using prior analysis and had insufficient descriptions of information such as the convergence conditions during the computation process (Cheng et al., 2007a, 2007b, Khajehzadeh et al., 2012). These researchers proposed an improved version of PSO as a modified PSO method, in which the computational efficiency is improved by updating weighting factors depending on the number of iterations. However, the proposed modified PSO has flaws, such as an increase in the number of analysis parameters.

This paper presents a simple slip surface search algorithm based on the PSO that improves convergence performance without increasing the number of analysis parameters. The proposed search algorithm adopts uniform random numbers to effectively search for the critical slip surface, to set a practical convergence condition, and to increase the number of nodes in the critical slip surface, respectively. Fig. 1 depicts the procedure used by the proposed search algorithm. This procedure is explained in detail in the ensuing sections.

### 3.1. Preconditions

Before presenting the specific non-circular slip surface search method, in this section, the definition of the function expressing the topography and slip surfaces along with the slip surface generation conditions are first presented. As shown in Fig. 2, the function $y=t(x)$ expresses the land surface, the function $y=l(x)$ expresses a stratum boundary, the function $y=s(x)$ expresses the slip surface, and the function $y=h(x)$ expresses the lower limit of a region generating a slip surface.

The slip surface nodes are defined by $(x_i, y_i)\forall i$, $i=1\cdots n$, and the following constraint conditions are imposed on the $x$ coordinates of the slip surfaces at the slope toe and the slope top on the land surface:

$$x_{1,\,\min} \le x_1 \le x_{1,\,\max} \tag{1}$$

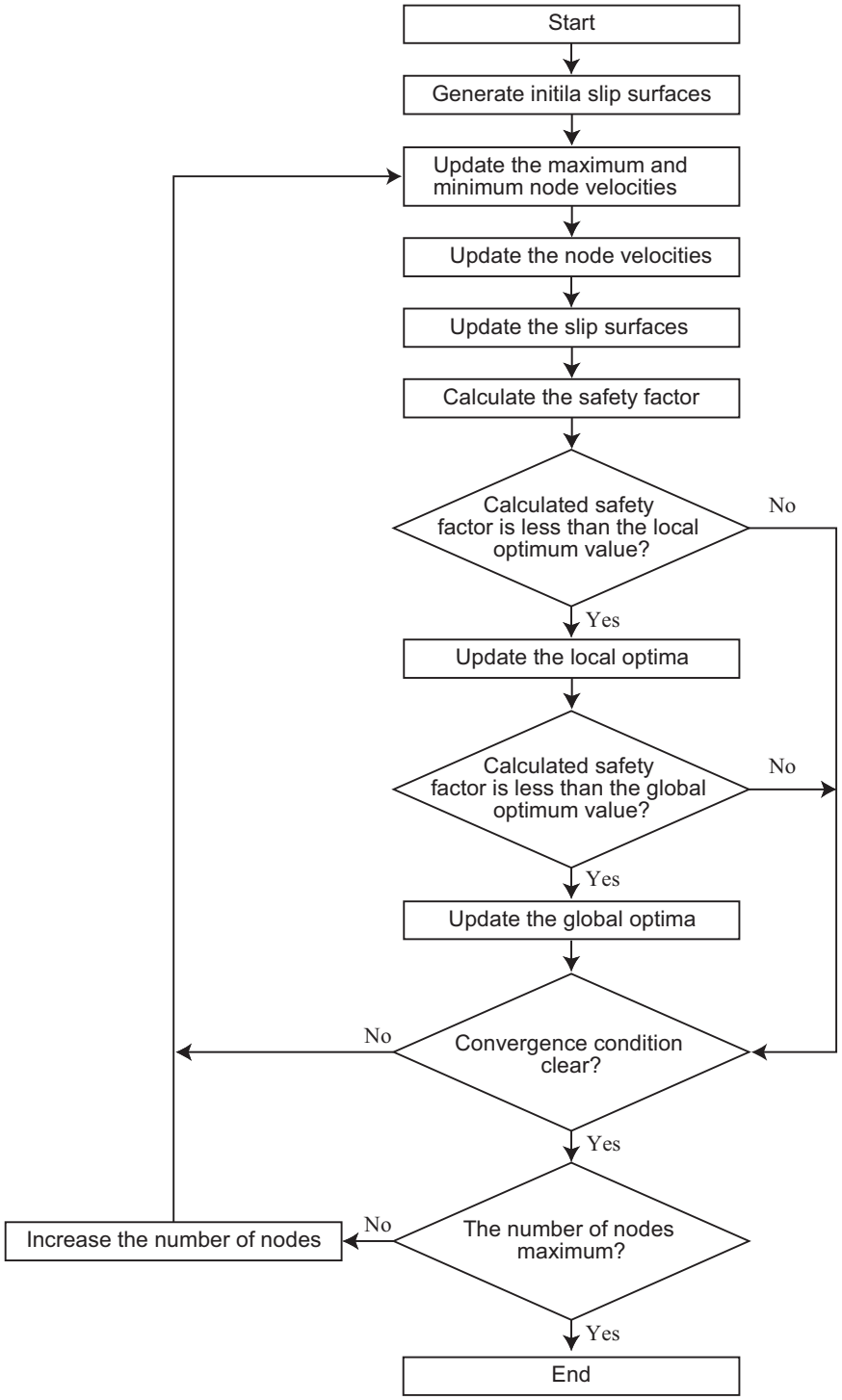


Fig. 1. Flow chart of the proposed algorithm to search a critical slip surface based on the particle swarm optimization (PSO) method.

$$x_{n,\,\min} \le x_n \le x_{n,\,\max} \tag{2}$$

Further, to generate a slip surface within an area having upper/lower limits, the following constraint condition is provided:

$$h(x) \le s(x) \le t(x) \tag{3}$$

For this condition, a group of coordinates configuring a given slip surface is defined as follows:

$$S = \{x_1, y_1, x_2, y_2, \cdots, x_n, y_n\} \tag{4}$$

The Spencer method is used to compute the safety factor in this paper. Thus, as shown below, the variables in the function used to find the safety factor are the slip coordinates ($S$) and the angle of inclination in between the slices ($\theta$).

$$FS = f(S, \theta) \tag{5}$$

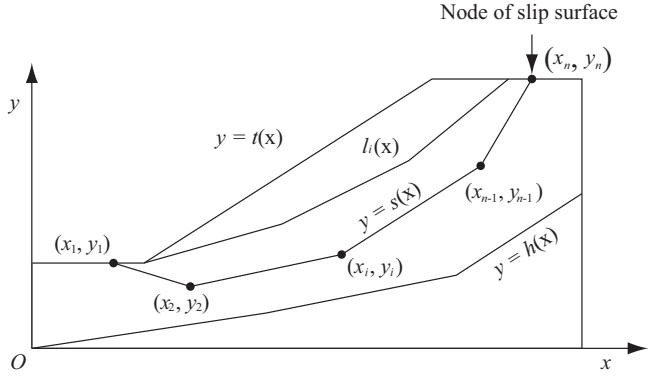


Fig. 2. Notations of the earth slope.

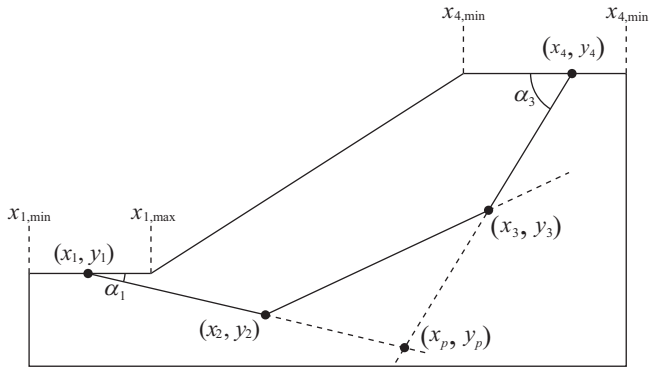


Fig. 3. Notations for setting the initial slip surface.

The non-circular slip surface search reduces to the problem of minimizing the goal function given by Eq. (5). Because this function is a multimodal function, it originates from the optimization problem of the multimodal function. In this paper, the following geometric constraint conditions are imposed on the generated slip surfaces:

$$x_i < x_{i+1} \forall i : i = 1 \cdots n-1 \tag{6}$$

$$y_i = t(x_i) \forall i : i = 1 \cdots n \tag{7}$$

$$h(x_i) < y_i \le t(x_i) \forall i : i = 2 \cdots n-1 \tag{8}$$

Because the PSO method is used here, for these conditions, the slip surface coordinates group of the $k$th step can be defined when multiple slip surface groups in the $k$th step are given by $S_j^k \forall j$: $j = 1 \cdots m$ as follows:

$$S_j^k = \{S_1^k, S_2^k, \cdots, S_m^k\} \tag{9}$$

where $S_1^k$ (for example) can be defined as follows:

$$S_1^k = \left\{x_{1,1}^k, y_{1,1}^k, x_{1,2}^k, y_{1,2}^k, \cdots, x_{1,n}^k, y_{1,n}^k\right\} \tag{10}$$

The slip surface coordinates groups are updated at each step in order to minimize the safety factor. The safety factor corresponding to each slip surface group is updated as follows:

$$FS\left(S_j^0\right) > FS\left(S_j^1\right) > \cdots > FS\left(S_j^k\right) > FS\left(S_j^{k+1}\right) \cdots \tag{11}$$

### 3.2. Generation of multiple initial slip surfaces

This paper adopts an algorithm to generate multiple initial slip surfaces from the research by Greco (1996). The $x$ coordinates of the slip surfaces at the slope toe and the slope top are defined as shown below, with the number of initial slip surface nodes set to four, $R_1$, $R_2$,…, where $R_n$ is a uniform random number in the interval [0, 1], as shown in Fig. 3.

$$x_{j,1}^0 = \frac{x_{1,\,\min} + R_{j,1}(x_{1,\,\max} - x_{1,\,\min})}{4} \tag{12}$$

$$x_{j,4}^0 = \frac{x_{4,\,\min} + R_{j,4}(x_{4,\,\max} - x_{4,\,\min})}{4} \tag{13}$$

The low-discrepancy sequence (LDS) (Tezuka, 1995; Tamura and Shirakawa, 1999; Shinoda, 2007), which has an extremely high uniformity even at high dimensions, is used for the uniform random numbers above. (Note: all the uniform random numbers cited subsequently in this paper are from the low-discrepancy sequence.) The uniformity of the adopted LDS was verified by comparing it with the results obtained for a one-dimensional sample generated by a random generator (Matsumoto and Nishimura, 1998) with 500 simulations, as shown in Fig. 4. (Hereafter, the latter uniform random variable will be referred to as the conventional uniform random variable.) Fig. 4(a) and (b) depict histograms of the conventional uniform random variable and the LDS in (0, 1), respectively. From Fig. 4(a), it is evident that the uniformity of the conventional random variable is not guaranteed. However, as can be seen in Fig. 4(b), the quasi-random variable obtained from the LDS exhibits a high uniformity.

When the $x$ coordinates of slip surface nodes 1 and 4 are fixed as defined above, the $y$ coordinates of the slip surfaces at the slope toe and the slope top are uniquely fixed as follows:

$$y_{j,1}^0 = t\left(x_{j,1}^0\right) \tag{14}$$

$$y_{j,4}^0 = t\left(x_{j,4}^0\right) \tag{15}$$

Next, the angles formed by nodes 1 and 4 with the horizontal plane are set using uniform random numbers as follows:

$$\alpha_1 = -40.0 + 15.0R_5 \tag{16}$$

$$\alpha_3 = 45.0 + 15.0R_6 \tag{17}$$

The process given below is executed to determine nodes 2 and 3 of the slip surface. In other words, this process finds the $x_p$ coordinate of the intersection point $x$ of the slip surface obtained from slip surface node 1 and Eq. (16) and the slip surface obtained from slip surface node 4 and Eq. (17).

$$x_p = \frac{y_4 - y_1 + x_1 \tan \alpha_1 - x_4 \tan \alpha_3}{\tan \alpha_1 - \tan \alpha_3} \tag{18}$$

The $x$ and $y$ coordinates of slip surface nodes 2 and 3 are given as follows:

$$x_2 = x_1 + R_2\left(x_p - x_1\right) \tag{19}$$

$$y_2 = y_1 + (x_2 - x_1)\tan \alpha_1 \tag{20}$$

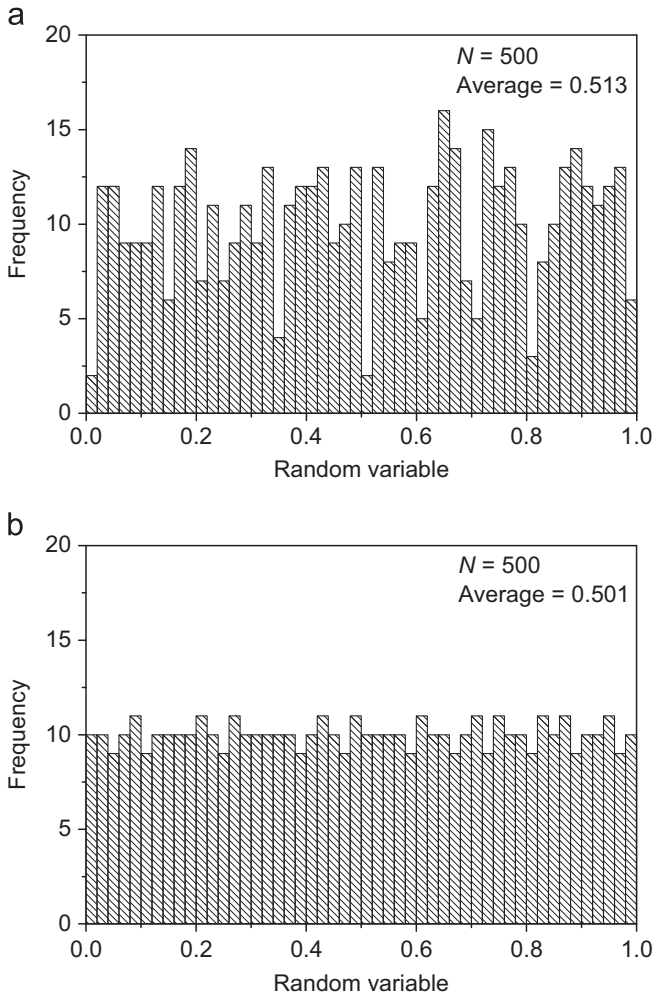


Fig. 4. Histogram of uniform random variable. (a) Conventional random variable. (b) Low-discrepancy sequence.

$$x_3 = x_4 - R_3\left(x_4 - x_p\right) \tag{21}$$

$$y_3 = y_4 + (x_3 - x_4)\tan\ \alpha_3 \tag{22}$$

### 3.3. Velocity computation and updating of slip surface coordinates

In order to generate slip surface nodes using the PSO method, the slip surface coordinates of the preceding step are updated by adding a velocity term, as shown in the following equations:

$$x_{j,i}^{k+1} = x_{j,i}^{k} + vx_{j,i}^{k+1} \tag{23}$$

$$y_{j,i}^{k+1} = y_{j,i}^{k} + vy_{j,i}^{k+1} \tag{24}$$

where $vx_{j,i}^{k+1}$ denotes the velocity in the $x$-direction and $vy_{j,i}^{k+1}$ denotes the velocity in the $y$-direction, which are given as follows:

$$vx_{j,i}^{k+1} = wvx_{j,i}^{k} + c_1 r_1 (xl_{j,i} - x_{j,i}^{k}) + c_2 r_2 (xg_i - x_{j,i}^{k}) \tag{25}$$

$$vy_{j,i}^{k+1} = wvy_{j,i}^{k} + c_1 r_3 (yl_{j,i} - y_{j,i}^{k}) + c_2 r_4 (yg_i - y_{j,i}^{k}) \tag{26}$$

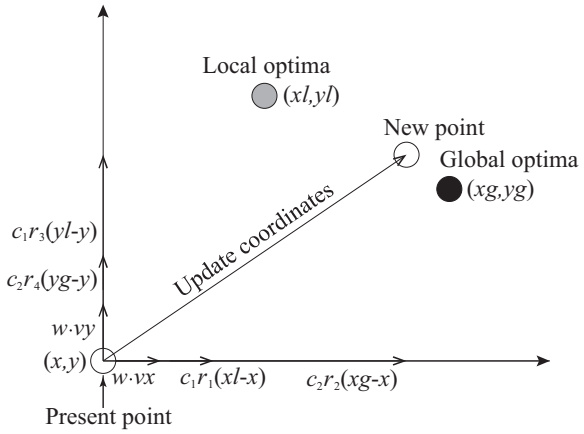


Fig. 5. Update nodes of the slip surfaces by the PSO method.

In the above equations, $w$ denotes the inertia weighting coefficient; $c_1$ indicates the local solution weighting coefficient; $c_2$ represents the optimum solution weighting coefficient; $r_1$ to $r_4$ denote uniform random numbers at the interval [0, 1]; $xl_{j,\ i}$ and $yl_{j,\ i}$ indicate the target particle's $x$-coordinate and $y$-coordinate local optimum solutions, respectively; and $xg_i$ and $yg_i$ denote the target particle's $x$-coordinate and $y$-coordinate global optimum solutions, respectively. In other words, as shown in Fig. 5, the new velocity is computed using the current particle velocity, its difference with the local optimum solution, and its difference with the global optimum solution. Here, the term "local optimum solution" implies the optimum solution for the target particle, and the term "global optimum solution" implies the optimum solution for all of the particles. For the computation of the velocities given by Eqs. (25) and (26), the following constraint conditions are imposed:

$$v_{j,i,\ \min}^{k} \le vx_{j,i}^{k} \le v_{j,i,\ \max}^{k} \tag{27}$$

$$v_{j,i,\ \min}^{k} \le vy_{j,i}^{k} \le v_{j,i,\ \max}^{k} \tag{28}$$

where $v_{j,i,\ \min}^{k}$ and $v_{j,i,\ \max}^{k}$ respectively denote the minimum and maximum values of the velocity calculated using the equations below. The minimum and maximum values of the velocity of the slip surface coordinate at the slope toe and the slope top are calculated as follows:

$$v_{j,1,\ \max}^{k+1} = \beta\left(x_{j,2}^{k} - x_{j,1}^{k}\right) \tag{29}$$

$$v_{j,1,\ \min}^{k+1} = -v_{j,1,\ \max}^{k+1} \tag{30}$$

$$v_{j,n,\ \min}^{k+1} = \beta\left(x_{j,n}^{k} - x_{j,n-1}^{k}\right) \tag{31}$$

$$v_{j,n,\ \max}^{k+1} = -v_{j,n,\ \min}^{k+1} \tag{32}$$

The minimum and maximum values of the velocity of the slip surface coordinates at positions other than the slope toe and the slope top are calculated as follows:

$$v_{i,\ \max}^{k+1} = \beta\left(x_{j,i+1}^{k} - x_{j,i}^{k}\right) \tag{33}$$

$$x_{i,\max}^{k+1} = \beta\left(x_{j,i}^{k} - x_{j,i-1}^{k}\right) \tag{34}$$

where $\beta$ denotes the parameter that determines the magnitude of the minimum and maximum values of the velocity; hence, in order to satisfy Eq. (6), it must be set to a value smaller than 0.5. Therefore, in this paper, a value of 0.4 is used.

### 3.4. Safety factor calculation and updating of local and global optimum solutions

In this paper, the Spencer method is used to compute the safety factor to satisfy the force equilibrium equation in the horizontal and vertical directions, and the moment equilibrium equation—which is based on the equilibrium equations presented by Furuya (1997) using the Spencer method. The vertical seismic intensity component is considered in the calculation of seismic stability and deformability of earth slope subjected to the horizontal and vertical seismic motions simultaneously. If a safety factor is computed with the updated slip surface coordinates, and a safety factor smaller than the local optimum solution or the global optimum solution is obtained, the slip surface coordinates in the local optimum solution or the global optimum solution have to be updated.

### 3.5. Convergence conditions

No clear convergence conditions for the PSO method have been proposed thus far. In some applications, the slope stability analysis is preset to the number of repetitions deemed likely to converge and the computation is repeated the preset number of times (Khajehzadeh et al., 2012), whereas others set a safety factor difference before and after a preset number of repetitions as the convergence condition (Cheng et al., 2007a). In this paper, the basic approach is to set the absolute value of the velocity term given by Eqs. (25) and (26), and the difference in the safety factor before and after the number of trials as the convergence conditions. The convergence conditions for the PSO method utilized in this paper are as follows:

$$\sqrt{vx_{j,i}^{k} + vy_{j,i}^{k}} < \varepsilon_v \forall i, \quad j : i = 1 \cdots n, \quad j = 1 \cdots m \tag{35}$$

and

$$\Delta FS < \varepsilon_{FS} \tag{36}$$

where $\varepsilon_v$ denotes the tolerance error of the velocity; $\Delta FS$, the difference in the safety factor before and after the number of trials; and $\varepsilon_{FS}$, the tolerance error of the safety factor. A prior analysis showed that as the length of the slip surface increased, the amount of movement that the slip surface coordinates had, which affected the safety factor, decreased (in other words, the safety factor was significantly changed by a slip surface coordinate movement of 0.1 m for a slip surface length of 1.0 m, and the safety factor was marginally changed by a slip surface coordinate movement of 0.1 m for a slip surface length of 10.0 m). Hence, $\varepsilon_v$ was set in accordance with the length of the slip surface. In this paper, the value is set to equal the length of the slip surface divided by 1500. Further, a value of 0.0001 is used for $\varepsilon_{FS}$. When the PSO method is used, the velocity term given in Eqs. (25) and (26) may be slow to converge or may not converge, depending on the parameter values. Therefore, in addition to the convergence conditions mentioned above, the proposed method sets an upper limit value for the number of trials for each maximum number of nodes. In this paper, 200 is set as the upper limit for the number of repetitions on the basis of prior analysis.

### 3.6. Increasing numbers of nodes

If the safety factor converges with the current number of slip surface nodes, and the number of slip surface nodes does not satisfy the target number of slip surface nodes, the number of slip surface nodes is increased in accordance with the method described by Greco (1996), as shown below. First, the current slip surface node number is updated as follows:

$$x_{j,2i-1}^{k+1} = x_{j,i}^{k} \forall i : i = 1 \cdots n \tag{37}$$

$$y_{j,2i-1}^{k+1} = y_{j,i}^{k} \forall i : i = 1 \cdots n \tag{38}$$

Next, the maximum number of slip surface nodes is increased as follows:

$$n = 2n - 1 \tag{39}$$

Finally, a new node is set between the slip surface nodes updated by Eqs. (37) and (38) as follows:

$$x_{j,i}^{k} = \frac{x_{j,i-1}^{k} + x_{j,i+1}^{k}}{2} \forall i : i \bmod 2 = 0 \tag{40}$$

$$y_{j,i}^{k} = \frac{y_{j,i-1}^{k} + y_{j,i+1}^{k}}{2} \forall i : i \bmod 2 = 0 \tag{41}$$

As described previously, the initial maximum number of slip surface nodes is four; therefore, the maximum number of slip surface nodes will range over the values four, seven, 13, 25, and onwards.

## 4. Newmark's sliding block analysis with non-circular slip surface

In this paper, Newmark analysis is adopted for permanent seismic displacement analysis dealing with a non-circular slip surface. In the conventional Newmark analysis, the permanent seismic displacement of earth slopes subjected to a strong ground motion is calculated by integrating the equation of rotational motion of a soil mass contained within the critical circular slip surface by assuming the failure mass as a rotational rigid block (Shinoda et al., 2006). The equation of rotational motion is solved for the rotation caused by the difference between the driving and resisting moments. The critical slip surface is determined by the conventional stability analysis using a specific acceleration or seismic coefficient to yield a safety factor of 1.0. (Hereafter, this acceleration and

seismic coefficient will be referred to as the yield acceleration and the yield seismic coefficient, respectively.)

The solution to the permanent seismic displacement by the proposed Newmark analysis method dealing with the non-circular slip surface is similar to that of the conventional Newmark analysis method. The difference lies in the derivation of the equation governing the horizontal and vertical motion of the soil mass contained within the critical non-circular slip surface. The equations governing horizontal and vertical motions are solved for the movement caused by the difference between the driving and resisting forces. The calculation procedure is explained in detail below.

### 4.1. Calculation of yield seismic coefficients

When considering the ground motion in both the horizontal and vertical directions, a unique combination of the yield seismic coefficients of the vertical and horizontal directions cannot be determined under the condition of a safety factor equal to 1.0. Therefore, the yield seismic coefficients in both the horizontal and vertical components can be obtained from the convergence calculation using the two points across the safety factor equal to 1.0 when the safety factor first becomes smaller than 1.0 from the start of the time history. The yield seismic coefficient of the earth slopes subjected to only horizontal or vertical seismic motion can simply be calculated without considering the time history of acceleration (see Shinoda et al. (2006) for the calculation of yield seismic coefficient).

### 4.2. Calculation of permanent seismic displacements

#### 4.2.1. Calculation of permanent seismic displacement in the horizontal and vertical components

The equation of motion in the slice $i$ in the horizontal and vertical directions can be derived as follows:

$$\frac{W_i}{g}\ \ddot{X}_i = F_{X\,i} \tag{42}$$

$$\frac{W_i}{g}\ddot{Y}_i\ = F_{Y\,i} \tag{43}$$

where $\ddot{X}_i$ and $\ddot{Y}_i$ are the horizontal and vertical accelerations in the slice, and $F_{Xi}$ and $F_{Yi}$ are summations of the horizontal and vertical forces. The equations of motion in the center of the gravity of the sliding soil mass can be derived from Eqs. (42) and (43) as follows:

$$\sum_{i=1}^{n}\frac{W_i}{g}\ \ddot{X}_G = \sum_{i=1}^{n} F_{X\,i} \tag{44}$$

$$\sum_{i=1}^{n}\frac{W_i}{g}\ddot{Y}_G\ = \sum_{i=1}^{n} F_{Y\,i} \tag{45}$$

where $X_G$ and $Y_G$ are the horizontal and vertical displacements of the center of gravity in the sliding soil mass, which can be calculated by the linear acceleration method as follows:

for the horizontal component;

$$\ddot{X}_{G,t+\Delta t} = \frac{\sum_{i=1}^{n} F_{Xi}}{\sum_{i=1}^{n} W_i} g \tag{46}$$

$$\dot{X}_{G,t+\Delta t} = \dot{X}_{G,t} + \frac{1}{2}\left(\ddot{X}_{G,t} + \ddot{X}_{G,t+\Delta t}\right)\Delta t \tag{47}$$

$$X_{G,t+\Delta t} = X_{G,t} + \dot{X}_{G,t}\Delta t + \frac{1}{6}\left(2\ddot{X}_{G,t} + \ddot{X}_{G,t+\Delta t}\right)\Delta t^2 \tag{48}$$

for the vertical component;

$$\ddot{Y}_{G,t+\Delta t} = \frac{\sum_{i=1}^{n} F_{Yi}}{\sum_{i=1}^{n} W_i} g \tag{49}$$

$$\dot{Y}_{G,t+\Delta t} = \dot{Y}_{G,t} + \frac{1}{2}(\ddot{Y}_{G,t} + \ddot{Y}_{G,t+\Delta t})\Delta t \tag{50}$$

$$Y_{G,t+\Delta t} = Y_{G,t} + \dot{Y}_{G,t}\Delta t + \frac{1}{6}\left(2\ddot{Y}_{G,t} + \ddot{Y}_{G,t+\Delta t}\right)\Delta t^2 \tag{51}$$

The horizontal and vertical displacements of the center of gravity in the sliding soil mass are calculated as zero when the velocities defined by Eqs. (47) and (50) become zero or have negative values.

#### 4.2.2. Calculation of permanent seismic displacement in the rotational component

Similar to the derivation of the equation of horizontal and vertical motions, the equation of rotational motion about $O_c$ can be derived as follows:

$$-\left(\sum_{i=1}^{n} W_i\left({x_{oi}}^2 + {y_{oi}}^2\right)\right)\ddot{\theta}_c = \sum_{i=1}^{n} MR_i^* \tag{52}$$

The notations are defined in Fig. 6, where $x_{oi}$ and $y_{oi}$ are the horizontal and vertical distances between $O_c$ and the center of the bottom of the slice; $\ddot{\theta}_c$ is the angular acceleration about $O_c$;

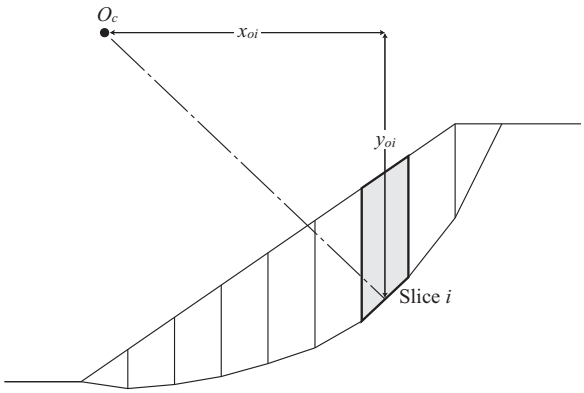


Fig. 6. Notations of the earth slope in the rotational motion.

$MR_i^*$ is the summation of moments about $O_c$ when the safety factor first becomes 1.0 during seismic motion. The rotation about $O_c$ can be calculated by the linear acceleration method as follows:

$$\ddot{\theta}_c = -\sum_{i=1}^{n} MR_i^* \Big/ \left( \sum_{i=1}^{n} W_i \left( {x_{oi}}^2 + {y_{oi}}^2 \right) \right) \tag{53}$$

$$\dot{\theta}_{c,t+\Delta t} = \dot{\theta}_{c,t} + \frac{1}{2} \left( \ddot{\theta}_{c,t} + \ddot{\theta}_{c,t+\Delta t} \right) \Delta t \tag{54}$$

$$\theta_{c,t+\Delta t} = \theta_{c,t} + \dot{\theta}_{c,t} \Delta t + \frac{1}{6} \left( 2\ddot{\theta}_{c,t} + \ddot{\theta}_{c,t+\Delta t} \right) \Delta t^2 \tag{55}$$

#### 4.2.3. Calculation of permanent seismic displacement

The permanent seismic displacements by the proposed method can be calculated with horizontal, vertical, and rotational components. Their values are selected considering the shape of the slip surface. For example, when the slip surface is circular, the permanent seismic displacement should be calculated from the rotational component. On the other hand, when the slip surface is non-circular, the resultant permanent seismic displacement should be calculated from the horizontal and vertical components. The rotational and resultant permanent seismic displacements can be calculated as follows:

$$d_{\theta i} = \theta_c \sqrt{{x_{oi}}^2 + {y_{oi}}^2} \tag{56}$$

$$ds = \sqrt{{X_G}^2 + {Y_G}^2} \tag{57}$$

## 5. Validity verification

### 5.1. Stability analysis with the PSO-based critical slip surface search method

Example 1 is used to verify the seismic safety factor obtained by the proposed method. As a means of verification, the seismic safety factor obtained by the proposed method is compared with that previously obtained by other researchers. Fig. 7 and Table 1 show the analytical model and the soil properties of Example 1. This model has four layers, including a weak layer that is expected to cross the critical slip surface. The geometric configuration of the analytical model in Example 1 is virtually the same as that by Zolfaghari et al. (2005) and Cheng et al. (2007a) except for the boundary condition of the backfill. In Example 1, the boundary of the backfill soil is extended to search the deep critical slip surface in the seismic condition. The soil properties of the analytical model reported by Zolfaghari et al. (2005) and Cheng et al. (2007a) differed as a result of unit conversion. Therefore, the soil property in the analytical model reported by Cheng et al. (2007a) was adopted in the current analysis.

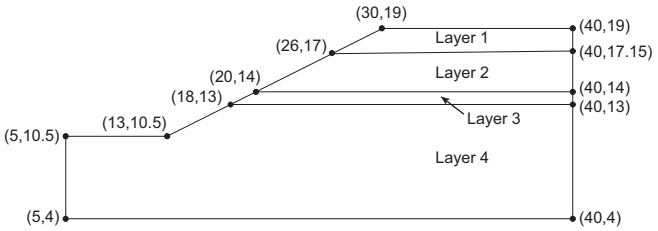


Fig. 7. Analytical model of earth slope of Example 1.

In the example, the horizontal seismic coefficient was 0.1. In order to exclude any inappropriate critical slip surface from the current analysis, the minimum and maximum values were set at the slip surface of the $x$ coordinates of the slope toe and the slope top for the setting of the land surface slip surface coordinates. An area with $x$ coordinates from 15.0 to 25.0 at the slope toe and $x$ coordinates from 30.0 to 45.0 at the slope top was set as the slip surface generation area.

As described earlier, the value set for the tolerance error of the node velocity was the slip surface length divided by 1500, and the value set for the safety factor tolerance error was 0.0001. The number of slip surface nodes was initially four, then it subsequently increased to seven, and then 13. The number of particle swarms used in the current PSO method was 40. When the PSO method was used to evaluate the local and global optimum solutions after generating 40 slip surfaces simultaneously, the number of trials was counted as one trial at the point in time when 40 slip surfaces were generated. In other words, the number of safety factor calculations was equal to the number of simulations multiplied by the number of particle swarms. The weighting coefficient of the PSO method were set as $w=0.65$, $c_1=1.2$, and $c_2=1.2$, as given by Wakasa et al. (2010). The sensitivity of the parameters of the PSO method for the precision and the convergence of the solutions are outside the scope of this paper; however, the findings in this area will be published in the near future.

Fig. 8 shows a plot of the seismic safety factor versus the number of simulations of the proposed method. When the

Table 1
Soil properties for Example 1.

| Layer | Unit weight (kN/m$^3$) | Cohesion (kPa) | Friction angle (deg.) |
|---|---|---|---|
| 1 | 19.0 | 15.0 | 20.0 |
| 2 | 19.0 | 17.0 | 21.0 |
| 3 | 19.0 | 5.0 | 10.0 |
| 4 | 19.0 | 35.0 | 28.0 |

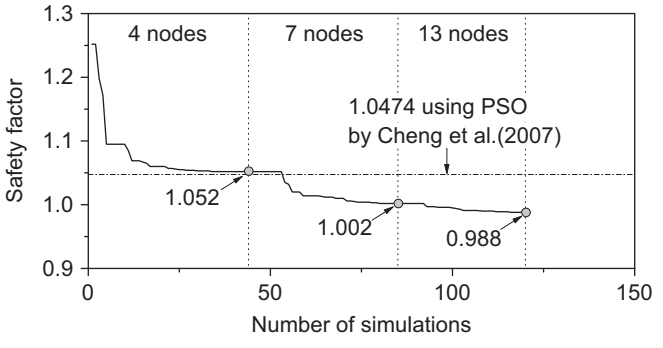


Fig. 8. Bias of safety factor calculation with the number of simulations by the proposed method.

Table 2
Comparison of safety factors and number of safety factor calculations obtained by the various optimization methods for Example 1.

| Optimization method | Literature | Method of safety factor calculation | Safety factor | Number of safety factor calculation |
|---|---|---|---|---|
| GA | Zolfaghari et al. (2005) | M–P | 1.37 | Unknown |
| Ant-colony | Cheng et al. (2007a) | Spencer | 1.3028 | 109,800 |
| Tabu | Cheng et al. (2007a) | Spencer | 1.1858 | 63,796 |
| SA | Cheng et al. (2007a) | Spencer | 1.1334 | 108,542 |
| SHM | Cheng et al. (2007a) | Spencer | 1.0733 | 99,831 |
| MHM | Cheng et al. (2007a) | Spencer | 1.0578 | 40,476 |
| PSO | Cheng et al. (2007a) | Spencer | 1.0474 | 69,600 |
| Present study | | Spencer | 0.970 | 4800 |

*Note*: GA = Genetic algorithm; Tabu = Tabu search; SA = Simulated annealing; SHM = Simple harm ony search; MHM = Modified harmony search; M–P = Morgenstern and Price method.

maximum numbers of slip surface nodes are four, seven, and 13, the number of simulations until the convergence are 44, 85, and 120, respectively. The fact that the number of simulations does not reach the upper limit of 200 indicates good convergence each time. The safety factors at the convergence for each maximum number of slip surface nodes were 1.052, 1.002, and 0.988, respectively.

Table 2 shows the seismic safety factors obtained by Zolfaghari et al. (2005), Cheng et al. (2007a), and the proposed method. The safety factor results obtained by Cheng et al. (2007a) using the PSO method is smaller than that obtained by the other methods, including the method by Zolfaghari et al. (2005), as shown in Table 2. However, the safety factor calculated by the proposed method is slightly smaller than that by Cheng et al. (2007a) using the PSO method. Moreover, the number of safety factor calculations in the proposed method is the smallest among that of all the methods, as shown in Table 2. As a representative result, Cheng et al. (2007a) reported the safety factor of the PSO method as 1.0474, with the number of safety factor computations at 69,600. In contrast, the safety factor calculated by the proposed method is 0.970, with the number of safety factor calculations at 4800 (i.e., $120 \times 40$). Fig. 9 compares the critical slip surface obtained by the proposed method with the slip surfaces obtained by the GA and PSO methods, as given in Table 2. The slip surface obtained by the proposed method, as shown in Fig. 9, is virtually the same as that by the PSO method reported by Cheng et al. (2007a), except for the tip of the slip surface. These findings verify that the analytical precision of the proposed method is valid for Example 1, and its computation efficiency is relatively higher than that of the existing methods.

These findings indicate that the safety factor obtained by the proposed method is marginally smaller than that of the existing methods, and its computation precision is relatively higher.

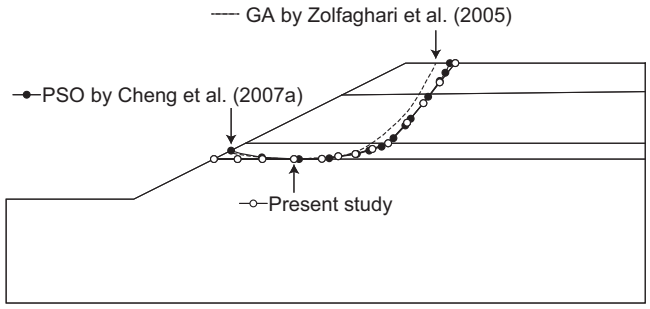


Fig. 9. Comparison of critical slip surface for Example 1.

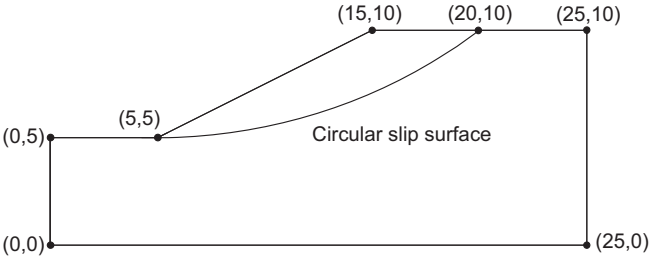


Fig. 10. Analytical model and determined circular slip surface of earth slope of Example 2.

### 5.2. Newmark analysis with circular critical slip surface

Verification of Newmark analysis with non-circular slip surface derived from the Spencer method was also conducted. According to an analytical condition, the safety factor of the earth slope with the circular slip surface by the Fellenius method is equal to that by the Spencer method. This indicates that the permanent seismic displacement of the earth slope with the circular slip surface by the Fellenius method is equal to that by the Spencer method. Therefore, a program to calculate the permanent seismic displacement of an earth slope by the Fellenius method (Shinoda et al., 2006) was used for comparison purposes with that obtained by the proposed method.

Fig. 10 shows the analytical model and the circular slip surface for Example 2. The geometric configuration of the analytical model in this paper is the same as that by Yamagami and Ueta (1988) and Greco (1996); however, the soil properties of the adopted analytical model were changed from the above previous research in which the unit weight and friction angle were 17.64 kN/m$^3$ and zero, respectively. This is because the permanent seismic displacement cannot be calculated because of the safety factor of less than 1.0 in the static condition. The five friction angles of the analytical model were determined to become yield seismic coefficients of 0.1, 0.15, 0.2, 0.25, and 0.3 by trial calculation. The circular slip surface was set in the center of the circular slip surface at (5.0, 30.9) and the radius as 25.0 m to pass through the toe of the earth slope of (5.0, 5.0).

Fig. 11 shows the horizontal ground motion in the NS direction arranged from seismic records observed at the Kiban – Kyoshin Net (KiK-net) Hino during the Western Tottori prefecture Earthquake in 2000. The amplitude of the

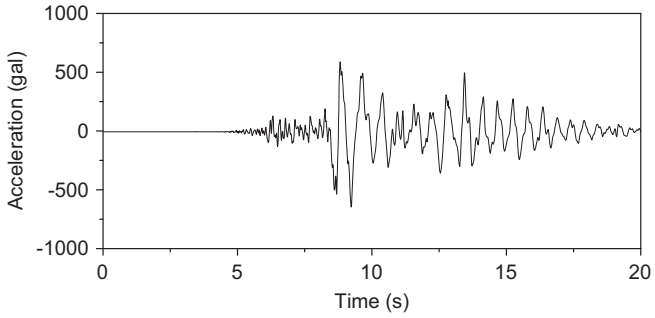


Fig. 11. Arranged ground motion in the NS direction of Western Tottori prefecture Earthquake in 2000.

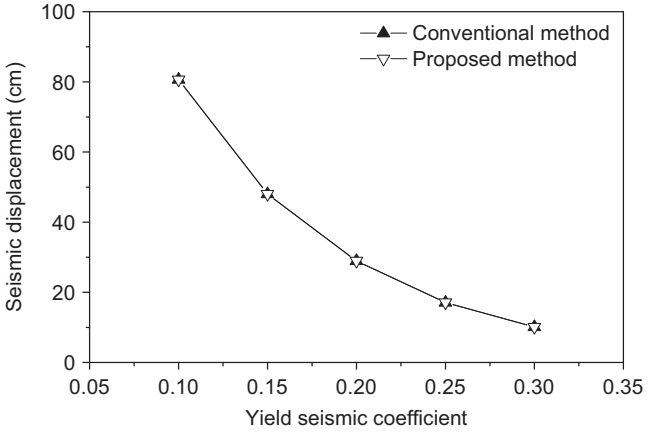


Fig. 12. Comparison of permanent seismic displacement with the yield seismic coefficient by the conventional and proposed methods of Example 2.

above ground horizontal motion was arranged to become an Arias intensity of 1000 m/s obtained from the ground horizontal and vertical motions. The maximum horizontal acceleration in the NS direction was 647 gal. This observed ground motion was used in the current analysis. The Arias intensity $I_A$ (Arias, 1970), a measure of the earthquake intensity, is obtained by integrating the squared accelerations over time as follows:

$$I_A = \frac{\pi}{2g}\int_0^{T_d}\{x(t)^2 + y(t)^2\}dt \tag{1'}$$

where $t$ is the time; $g$ is the acceleration due to gravity; $T_d$ is the duration of the ground motion; and $x(t)$ and $y(t)$ are the time histories of the horizontal and vertical accelerations, respectively. $I_A$ is a measure of the total acceleration of the record rather than of the peak only. It is therefore a better indicator of the magnitude of the shake than the peak ground acceleration.

Fig. 12 compares the permanent seismic displacements obtained from the conventional and proposed methods for Example 2. It can be clearly seen that both permanent seismic displacements are identical to the various yield seismic coefficients. Fig. 13 shows the time histories of the permanent seismic displacement obtained from the conventional and proposed methods under the yield seismic coefficient of 0.2.

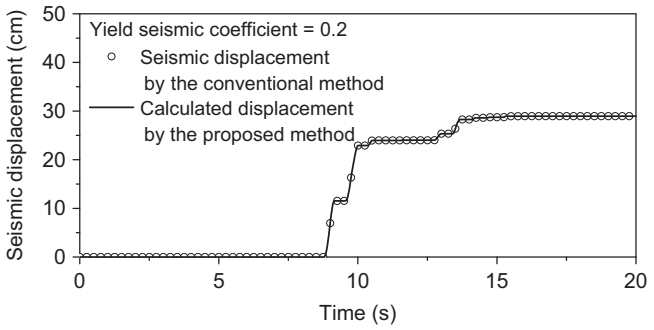


Fig. 13. Comparison of theoretical and calculated permanent seismic displacements of Example 2.

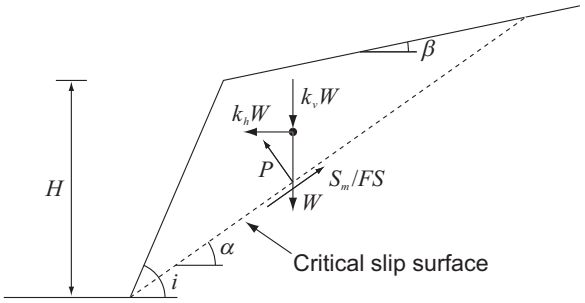


Fig. 14. Notations of the earth slope with planar failure surface.

It is also clearly shown that the time histories of the permanent seismic displacement by the conventional and proposed methods are identical. These analytical results verify that the proposed method can calculate the permanent seismic displacement of the earth slope with the critical circular slip surface.

### 5.3. Newmark analysis with planar critical slip surface

Evaluation of the seismic stability of the earth slope exhibiting a planar critical slip surface as well as the circular critical slip surface is important. To verify the proposed method in this case, the permanent seismic displacement obtained by the method was compared to that obtained by Culmann's analysis method presented by Francais (1820), which is considered a theoretical solution. Fig. 14 shows the forces acting on the earth slope exhibiting the planar critical slip surface, where $H$ is the slope height, $i$ is the slope inclination, $\alpha$ is the inclination of the planar critical slip surface, $\beta$ is the inclination of backfill of the slope, and $k_h$ and $k_v$ are horizontal and vertical seismic coefficients, in which the positive $k_v$ is considered to act downwards in this paper. $W$ is the weight of the sliding soil mass, which can be geometrically calculated as follows:

$$W = \frac{\gamma H^2}{2}\frac{\sin(i-\alpha)\sin(i-\beta)}{\sin(\alpha-\beta)\sin^2 i} \tag{58}$$

The equation of motion along the planar critical slip surface can be derived as follows:

$$\ddot{d}_t = \frac{\cos(\phi-\alpha)}{\cos\phi}(k_h - k_{hy})g \tag{59}$$

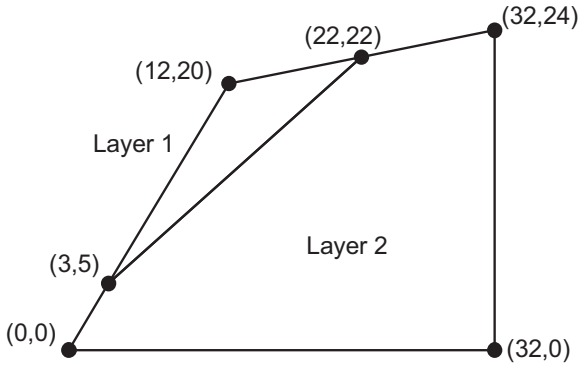


Fig. 15. Analytical model of earth slope of Example 3.

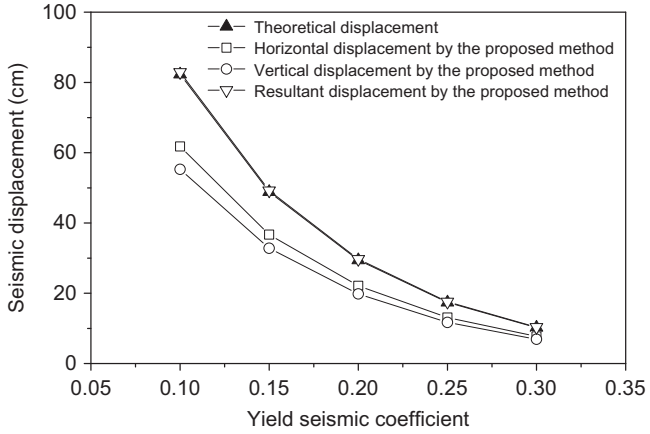


Fig. 16. Comparison of theoretical and calculated permanent seismic displacements plotted against the yield seismic coefficient of Example 3.

where $d_t$ is the permanent seismic displacement, which can be theoretically calculated as follows:

$$d_t = \frac{\cos(\phi-\alpha)}{\cos\phi} \iint (k_h - k_{hy})\, g\, dt \tag{60}$$

where $k_{hy}$ is the yield seismic coefficient, which can be calculated as follows:

$$k_{hy} = \frac{cl\cos\phi - (1+k_v)W\sin(\alpha-\phi)}{W\cos(\alpha-\phi)} \tag{61}$$

For the calculation of the permanent seismic displacement in Eq. (60), the velocity obtained from Eq. (59) was set to zero when the above velocity became a negative value.

Fig. 15 shows the analytical model for Example 3, in which the earth slope model exhibited a planar critical slip surface. The unit weight and friction angle of the upper and lower layers werere 19.5 kN/m$^3$ and 20°. The cohesion of the lower layer was set at a high value not to cross the critical slip surface in the lower layer. The several cohesions of the upper layer were determined to become yield seismic coefficients of 0.1, 0.15, 0.2, 0.25, and 0.3 by trial calculation. The planar critical slip surface was set to cross the two points (3, 5) and (22, 22). The same seismic motion as that in Example 2 was used for the permanent seismic displacement calculation, as shown in Fig. 11.

Fig. 16 compares the permanent seismic displacements obtained from the theoretical and proposed methods. The resultant displacement by the proposed method can be calculated from the horizontal and vertical displacements shown in Fig. 16. It is clearly shown that both permanent seismic displacements are identical to the various yield seismic coefficients. Fig. 17 shows time histories of the permanent seismic displacement obtained from the theoretical and proposed methods under the yield seismic coefficient of 0.2. It is also clearly shown that the time histories of the permanent seismic displacement by the theoretical and proposed methods are identical. These analytical results verify that the proposed method can calculate permanent seismic displacement of earth slopes with the planar critical slip surface.

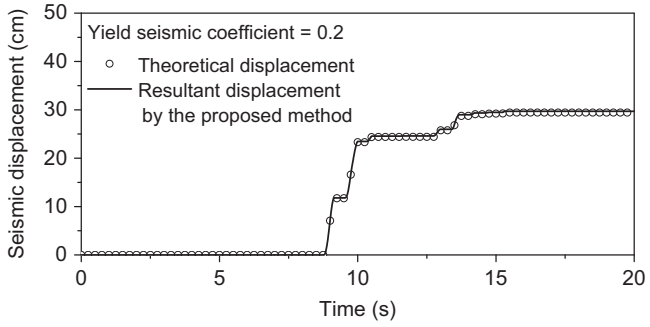


Fig. 17. Theoretical and calculated time histories of permanent seismic displacement of Example 3.

## 6. Application of Newmark analysis with non-circular slip surface

This section verifies the applicability of the proposed method to the seismic stability and deformability of earth slopes subjected to seismic loading in both the horizontal and vertical directions. The geometry of the analytical model of Example 4 is the same as that of Example 1, shown in Fig. 7. The geometric configuration and soil properties of the analytical model in this paper are the same as that by Zolfaghari et al. (2005) except for the boundary condition of the backfill and cohesion of the third layer. The cohesion of the third layer was determined to become the yield seismic coefficients 0.1, 0.2, and 0.3 by trial calculation. The ground motions observed, including both the horizontal and vertical acceleration, are used in the current analysis. Fig. 18 shows a vertical ground motion in the UD direction arranged from the seismic record observed at the Kiban–Kyoshin Net (KiK-net) Hino during the Western Tottori prefecture Earthquake in 2000. As mentioned before, the amplitude of the above ground vertical motion was arranged to become an Arias intensity of 1000 m/s obtained from the ground horizontal and vertical motions, in which the maximum vertical acceleration was 580 gal.

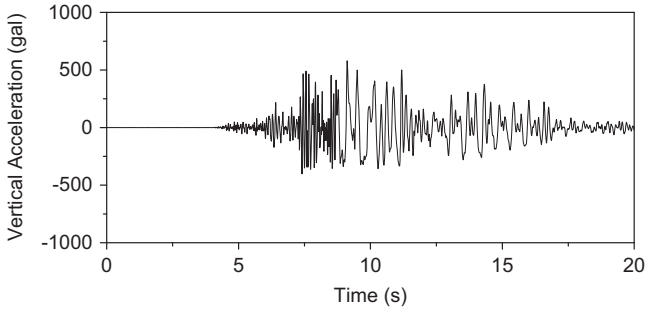


Fig. 18. Arranged ground motion in the UD direction of Western Tottori prefecture Earthquake in 2000.

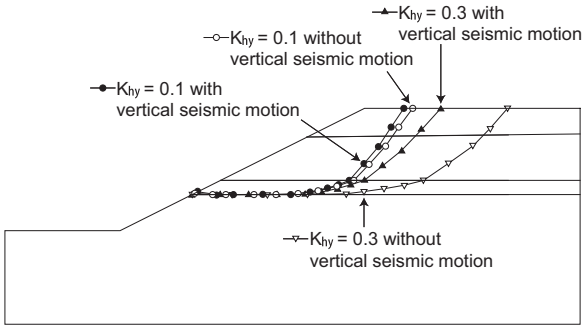


Fig. 19. Critical slip surface with and without vertical seismic motion of Example 4.

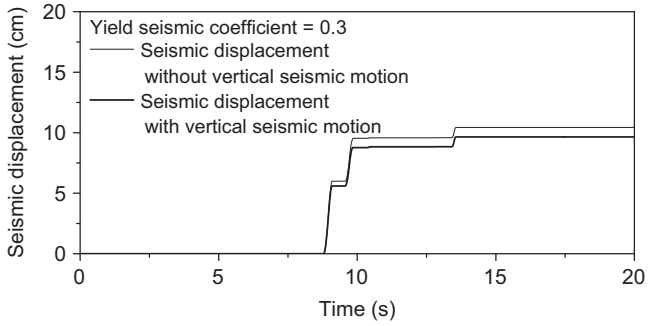


Fig. 20. Time histories of the permanent seismic displacement of the earth slope subjected to horizontal seismic motion with and without vertical seismic motions of Example 4.

Fig. 19 shows the non-circular critical slip surfaces obtained from calculations with yield seismic coefficients of 0.1 and 0.3, with and without vertical seismic motions. From the calculations, there is a trend to exhibit the deeper critical slip surface to increase the yield seismic coefficient, as shown in Fig. 19. Under the same horizontal yield seismic coefficient, the critical slip surface in the case with vertical seismic motion is shallower than that without the vertical seismic motion. Fig. 20 compares the time histories of the permanent seismic displacements of the earth slope model subjected to horizontal seismic motion with and without vertical seismic motion. Both permanent seismic displacements increase at the same time. This indicates that the trigger of the sliding of the earth slope depends on the horizontal inertia force in the current analytical

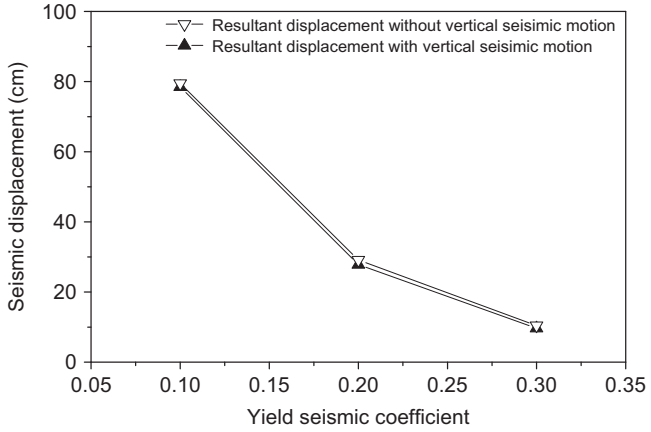


Fig. 21. Comparison of the permanent seismic displacements with and without vertical seismic motion plotted against the yield seismic coefficient of Example 4.

model and seismic motion. Further, the permanent seismic displacement in the case without the vertical seismic motion is slightly larger than that with the vertical seismic motion. Fig. 21 compares the permanent seismic displacements of the earth slope model subjected to horizontal seismic motion, with and without vertical motions, with various horizontal yield seismic coefficients. In the various horizontal yield seismic coefficients, the effect of the vertical seismic motion on the calculation of the permanent seismic displacement in the current analytical model is likely to be small. The effect of the vertical seismic motion of the permanent seismic displacement should be investigated with various geometry and phase differences of horizontal and vertical seismic motions in the near future.

## 7. Conclusions

This paper described an efficient numerical technique to compute the safety factor of earth slopes that uses a non-circular critical slip surface search algorithm with a stability analysis. In order to search the non-circular critical slip surface, the PSO method was used in this analysis. This technique has an advantage over the previously published PSO methods and other search algorithms that converge local optima even when the simulation number is large, thereby inducing an impermissible numerical error. The proposed method is applicable to the calculation of the safety factor of the earth slopes under a smaller number of simulations.

A new numerical technique to compute the permanent seismic stability of earth slopes exhibiting a non-circular slip surface subjected to concurrent seismic forces in the vertical and horizontal directions was also proposed. The PSO method was used to search the non-circular critical slip surface in this analysis. The proposed method is applicable to the calculation of permanent seismic displacement of the earth slopes.

The permanent seismic displacement calculated by Newmark analysis is a very important index for evaluating the seismic performance of the earth slopes exhibiting linear or

circular critical slip surface. This is because the permanent seismic displacement calculated by the Newmark analysis is equivalent to the displacement along the critical slip surface. However, the permanent seismic displacement of the earth slope exhibiting non-circular slip surface is different from the displacement along the critical slip surface. The permanent seismic displacement calculated by the proposed method is an important index that can be used to evaluate the seismic performance of the earth slope quantitatively, which represents the soil property of the earth slope and the seismic motion.

Additional research is required to integrate the proposed method into the permanent seismic displacement calculation and consideration for the degradation of yield acceleration due to transition in the residual state and acceleration response in the earth slope. Further investigation of the effect of phase difference between the vertical and horizontal seismic motions on the permanent seismic displacement calculation is also important. For such an investigation, calculations which incorporate the various geometries of the earth slope with the observed seismic motions and relevant experimental model tests are necessary.

## References


Arias, A., 1970. A measure of earthquake intensity. In: Hansen, R.J. (Ed.), Seismic Design for Nuclear Power Plants. MIT Press, Cambridge, MA, pp. 438–489.

Bishop, A.W., 1954. The use of the slip circle in the stability analysis of slopes. Géotechnique 5 (1), 7–17.

Bray, J.D., Travasarou, T., 2007. Simplified procedure for estimating earthquake-induced deviatoric slope displacements. J. Geotech. Geoenviron. Eng. 133 (4), 381–392.

Cheng, Y.M., Li, L., Chi, S.C., 2007a. Performance studies on six heuristic global optimization methods in the location of critical slip surface. Comput. Geotech. 34 (6), 462–484.

Cheng, Y.M., Li, L., Chi, S.C., Wei, W.B., 2007b. Particle swarm optimization algorithm for the location of the critical non-circular failure surface in two-dimensional slope stability analysis. Comput. Geotech. 34 (2), 92–103.

Fellenius, W., 1936. Calculation of the stability of earth dams. In: Proceedings of the 2nd Congress on Large Dams, Washington, DC, vol. 4, pp. 445–462.

Francais, 1820. Recherches sur la Poussee des Terres sur la Forme et lesDimensions des Murs de Revetment et sur les Talus d'Excavation, Paris.

Furuya, T., 1997. Consideration on the Spencer's general limit equilibrium method of slices. J. Jpn. Landslide Soc. 34 (2), 35–41 (in Japanese).

Goh, A.T., 1999. Genetic algorithm search for critical slip surface in multiple-wedge stability analysis. Can. Geotech. J. 36 (2), 359–382.

Goodman, R.E., Seed, H.B., 1966. Earthquake induced displacements of sand embankments. J. Soil Mech. Found., ASCE 92, 125–146.

Greco, V.R., 1996. Efficient Monte Carlo technique for locating critical slip surface. J. Geotech. Eng., ASCE 122 (7), 517–525.

Hyodo, M., Orense, R.P., Noda, S., Furukawa, S., Furui, T., 2012. Slope failures in residential land on valley fills in Yamamoto town. Soils Found. 52 (5), 975–986.

Janbu, N., 1955. Application of composite slip surface for stability analysis. In: Proceedings of the European Conference on Stability of Earth Slopes, vol. 3, pp. 43–49.

Japan Road Association (JRA), 2010. Guidelines for road earth works—slope works, Maruzenm (in Japanese).

Jibson, R.W., 2011. Methods for assessing the stability of slopes during earthquakes—a retrospective. Eng. Geol. 122, 43–50.

Kennedy, J., Eberhart, R., 1995. Particle swarm optimization. In: Proceedings of the 1995 IEEE International Conference on Neural Networks, pp. 1942–1948.

Khajehzadeh, M., Taha, M.R., El-Shafie, A., Eslami, M., 2012. Locating the general failure surface of earth slope using particle swarm optimisation. Civil Eng. Environ. Syst. 29, 41–57.

Kondo, K., Hayashi, S., 1997. Similarity and generality of the Morgenstern—-Price and Spencer methods. J. Jpn. Landslide Soc. 34 (1), 15–23 (in Japanese).

Koseki, J., Tatsuoka, F., Munaf, Y., Tateyama, M., Kojima, K., 1998. A modified procedure to evaluate active earth pressure at high seismic loads. Soils Found., special issue, 209–216.

Koseki, J., Koda, M., Matsuo, S., Takasaki, H., Fujiwara, T., 2012. Damage to railway earth structures and foundations caused by the 2011 off the Pacific Coast of Tohoku Earthquake. Soils Found. 52 (5), 872–889.

Kramer, S.L., 1996. Geotechnical Earthquake Engineering, N. J. Prentice Hall, Upper Saddle River.

Makdisi, F.I., Seed, H.B., 1978. Simplified procedure for estimating dam and embankment earthquake-induced deformations. J. Geotech. Eng. Div. 104 (7), 849–867.

Matasovic, N., Kavazanjian Jr., E., Yan, L., 1997. Newmark deformation analysis with degrading yield acceleration. Proc. Geosynth. 2 (97), 989–1000.

Matsumoto, M., Nishimura, T., 1998. A 623-dimensionally equidistributed uniform pseudorandom number generator. ACM Trans. Model. Comput. Simulat. 8 (1), 3–30.

Ministry of Land, Infrastructure and Transport (MLIT), 2005. Guidelines for seismic performance evaluation of dams during large earthquakes (Draft) (in Japanese).

Morgenstern, N.R., Price, V.E., 1965. The analysis of the stability of general slip surface. Géotechnique 15 (1), 79–93.

Newmark, N.M., 1965. Effects of earthquakes on dams and embankment. Géotechnique 15 (2), 139–160.

Pradel, D., Smith, P.M., Stewart, J.P., Raad, G., 2005. Case history of landslide movement during the Northridge earthquake. J. Geotech. Geoenviron. Eng. 131 (11), 1360–1369.

Railway Technical Research Institute (RTRI), 2000. Design Standard for Railway Earth Structures. Railway Technical Research Institute, Maruzen (in Japanese).

Sarma, S.K., Bhave, M.V., 1979. Stability analysis of embankments and slopes. J. Geotech. Eng. Div., ASCE 105 (12), 1511–1524.

Shinoda, M., Horii, K., Yonezawa, T., Tateyama, M., Koseki, J., 2006. Reliability-based seismic deformation analysis of reinforced soil slopes. Soils Found. 46 (4), 477–490.

Shinoda, M., 2007. Quasi-Monte Carlo simulation with low-discrepancy sequence for reinforced soil slopes. J. Geotech. Geoenviron. Eng., ASCE 133 (4), 393–404.

Shinoda, M., 2013a. Safety factor calculation of slopes by efficient search algorithm using noncircular slip surface. J. Jpn. Soc. Civil Eng., JSCE 69 (4), 432–443 (in Japanese).

Shinoda, M., 2013b. Calculation method of seismic residual displacement of slopes using Spencer's method. J. Jpn. Soc. Civil Eng., JSCE 69 (4), 491–503 (in Japanese).

Spencer, E., 1967. A method of analysis of the stability of embankments assuming parallel inter-slice forces. Géotechnique 17, 11–26.

Spencer, E., 1973. Thrust line criterion in embankment stability analysis. Géotechnique 23 (1), 85–100.

Tamura, T., Shirakawa, H., 1999. Quasi random numbers from generalized Faure sequences and their application to options evaluations. JAFEE J., 95–111 (in Japanese).

Tezuka, S., 1995. Uniform Random Numbers: Theory and Practice. Kluwer Academic Publishers, Boston.

Wakasa, Y., Tanaka, K., Akashi, T., 2010. Stability analysis of the particle swarm optimization algorithm,. Trans. Inst. Syst. Control Inform. Eng. 23 (1), 9–15.

Wartman, J., Bray, J.D., Seed, R.B., 2003. Inclined plane studies of the Newmark sliding block procedure. J. Geotech. Geoenviron. Eng. 129 (8), 673–684.

Wartman, J., Seed, R.B., Bray, J.D., 2005. Shaking table modeling of seismically induced deformations in slopes. J. Geotech. Geoenviron. Eng. 131 (5), 610–622.

Wasowsli, J., Keefer, D.K., Lee, C.-T., 2011. Toward the next generation of research on earthquake-induced landslide: current issues and future challenges. Eng. Geol. 122, 1–8.

Wilson, R.C., Keefer, D.K., 1983. Dynamic analysis of a slope failure from the 6 August 1979 Coyote Lake, California, earthquake. Bull. Seismol. Soc. Am. 73 (3), 863–877.

Yan, L., Matasovic, N., Kavazanjian E. Jr, 1996. Seismic response of a block on an inclined plane to vertical and horizontal excitation acting simultaneously. In: Proceedings of the 11th ASCE Engineering Mechanics Conference, pp. 1110–1113.

Yamagami, T., Ueta, Y., 1988. Search for noncircular slip surfaces by the Morgenstern – Price method. In: Proceedings of the 6th International Conference of Numerical Methods in Geomechanics, Innsbruck, pp. 1219–1223.

Zolfaghari, A.R., Heath, A.C., McCombie, P.F., 2005. Simple genetic algorithm search for critical non-circular failure surface in slope stability analysis. Comput.Geotech. 32, 139–152.